

Particle Tracking for Hadron Therapy with Plasma Panel Sensors: A Monte Carlo Simulation Study

Peter S. Friedman, *Member, IEEE*, Vladimir A. Bashkirov, *Member, IEEE*, and Reinhard W. Schulte, *Member, IEEE*

Abstract—Particle tracking technology is currently being explored with Monte Carlo simulation studies as well as first experimental prototypes as a method to improve the planning and delivery accuracy of hadron therapy. Advanced particle tracking technology is required to provide large-area detectors capable of single-particle registration at high data rates for applications such as particle imaging and pencil beam monitoring. One such candidate large-area particle tracking detector is based on plasma panel sensors (PPS). The PPS is an inherently digital, high gain, novel variant of micropattern gas detectors inspired by many operational and fabrication principles common to plasma display panels (i.e. plasma-TV's). The initial results of a simulation study of a realistic PPS telescope design shows that this technology is comparable to, or better than, existing silicon sensors in terms of both particle energy loss through the detector and spatial resolution for particle imaging. Further improvement of the track reconstruction accuracy is possible by reducing the PPS substrate thickness. Fabrication of the simulated PPS telescope is currently underway including thinner devices than those simulated.

I. INTRODUCTION

A JOINT DOE-NCI workshop on ion beam therapy (January 2013, Bethesda, MD) identified an ambitious set of technology developments needed to support a world-class treatment program for ion beam therapy. One important requirement is the ability to provide detectors that afford single-particle registration at high data rates with a high degree of uniformity and minimal interference with the particle beam. This would allow performing proton or ion CT prior to treatment and 2D/3D proton/ion radiography during treatment for integrated-range verification, along with beam diagnostics that have minimal interference with the primary beam. Current silicon detectors employed in first developments of proton imaging systems have major limitations in terms of maximum available detector size. Limitations also exist for currently used beam monitoring detectors that are not suitable for very fast response times at high beam intensities required for future clinical applications of particle beam scanning.

We are developing a novel detector, the plasma panel sensor (PPS), that has the potential to remove all the barriers

Manuscript received November 23, 2015. This work was supported by National Cancer Institute (NCI) grant 1R43 CA183437-01 from the NIH.

Peter S. Friedman is with Integrated Sensors, LLC, Ottawa Hills, OH 43606 USA (telephone: 419-536-3212, e-mail: peter@isensors.net).

Vladimir A. Bashkirov is with the Department of Basic Sciences, Division of Radiation Research, Loma Linda University, Loma Linda, CA 92354 USA (telephone: 909-558-4000, e-mail: vbashkirov@llu.edu).

Reinhard W. Schulte is with the Department of Basic Sciences, Division of Radiation Research, Loma Linda University, Loma Linda, CA 92354 USA (telephone: 909-558-4000, e-mail: rschulte@llu.edu).

of existing detectors and should therefore allow particle beam radiation therapy to realize its fullest potential to be used in future clinical particle beam therapy centers. Fundamentally, the proposed detectors should be inherently uniform and of low mass with fast response time. In the past year, we were successful in manufacturing ultrathin PPS substrates (i.e., 0.30 mm, 0.20 mm, and 0.026 mm thickness) with electrode pitches of 2.54 mm and 0.35 mm, corresponding to theoretical spatial resolutions of 0.73 mm and 0.10 mm, respectively, as demonstrated with Geant4 Monte Carlo simulations described in this paper. The simulation results indicate that sub-millimeter image resolution seems eminently achievable, and when combined with potentially high particle detection efficiencies could make these detectors the technology of choice for both imaging and beam monitoring sensors in the particle therapy treatment room of the future.

II. MONTE-CARLO MODEL OF THE PPS DETECTOR SYSTEM

The Geant4 [1] model of a realistic PPS structure with commercially available materials used in the simulation is shown in Fig. 1. It included the particle tracker consisting of two PPS panels installed in a gas-filled sealed chamber (20 cm x 20 cm x 10 cm) with ultrathin Ti entrance and exit windows (14 μm thick foils) and separated by 50 mm, a therapeutic proton beam line, and a water tank that stopped the beam. Each PPS panel comprised two 300 μm thick substrates made of glass-ceramic composition [2].

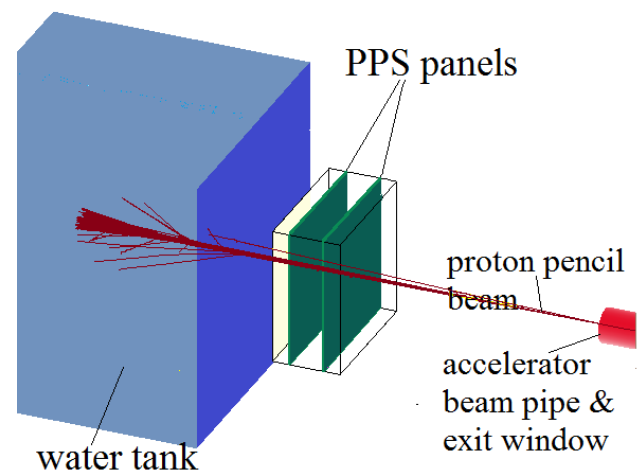


Fig. 1. Geant4 model of the PPS detector system installed in the proton beam line.

On the internal surfaces of the substrates, an identical hexagonal-patterned 30 μm wall structure composed of the same material as the glass-ceramic was deposited forming a hexagon pixel structure as shown in Fig. 2. In individual simulation runs, the detector pixel pitch P_c , defined by this structure, was set to 150 μm , 300 μm , and 500 μm , respectively.

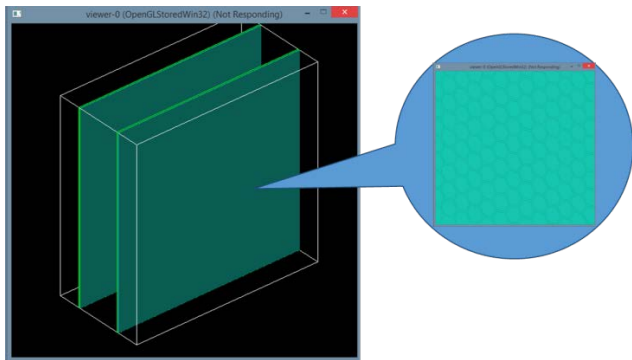


Fig. 2. Geant4 model of the PPS panels. The hexagon pixel structure is shown in the right insert.

Three gas mixtures: 90%CF₄ / 10%CO₂, 70%Ar / 30%CO₂, and 70%Ar / 30%CF₄ were simulated. The gas gap between the front and back substrates was 2 mm regardless of the pixel pitch, but the structure wall width varies with pixel pitch: for the pixel pitch of 500 μm , the walls occupy 10% of the area; for the 300 μm pitch this fraction is 15%, and for the 150 μm pitch it is 20%.

III. RESULTS OF THE MC SIMULATIONS

Results of the MC simulation with the Geant4 model of the PPS system, performed to study the PPS tracking performance for hadron therapy applications, are described in the following subsections A-D.

A. PPS response to protons and ions

The detection efficiency of an individual detector plane was inferred from the energy deposition (dE) in the 2 mm gas gap between the two PPS substrates by 200 MeV protons. The total number of ion-electron pairs was calculated as $N_{ip} = dE/W$, where W is the effective average energy to produce one ion pair (available from literature) – i.e., 26 eV for Ar, 36 eV for CF₄, and 33 eV for CO₂. The resulting ion-pair distributions for three different gas mixtures are shown in Fig. 3. The results show that for the 90%CF₄ / 10%CO₂ mixture the proton detection efficiency per panel should be very close to 100%, and for both other mixtures it should be better than 99%, assuming 100% avalanche probability if there are at least five ion-electron pairs on the particle track in the gas gap.

These results are for 200 MeV protons, and the efficiency should be practically 100% for protons of lower energy (e.g., traversing an imaging object), as well as for therapeutic ion beams. As an illustration of this statement, Fig. 4 shows the ion-pair distribution for a 375 MeV/n carbon ion beam. The carbon ion beam produces more than an order-of-magnitude

larger number of ion-electron pairs than the proton beam, and indicates that high registration efficiency can be achieved with a smaller working gas gap (e.g., 1 mm or even less), which would allow making the detector response faster.

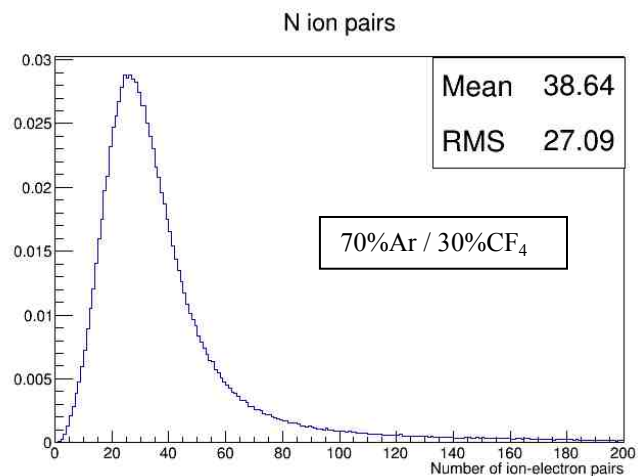
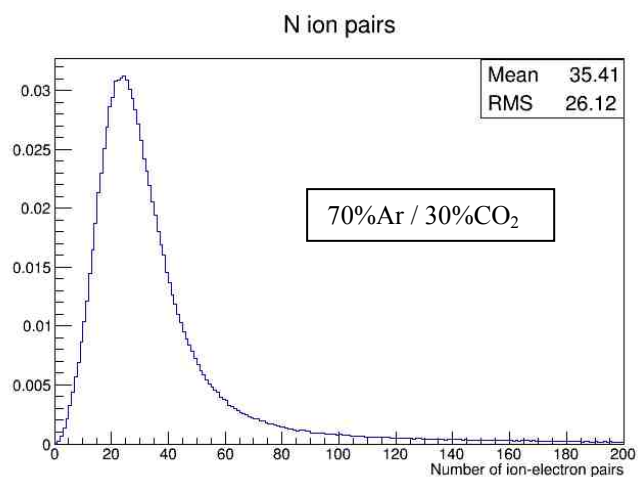
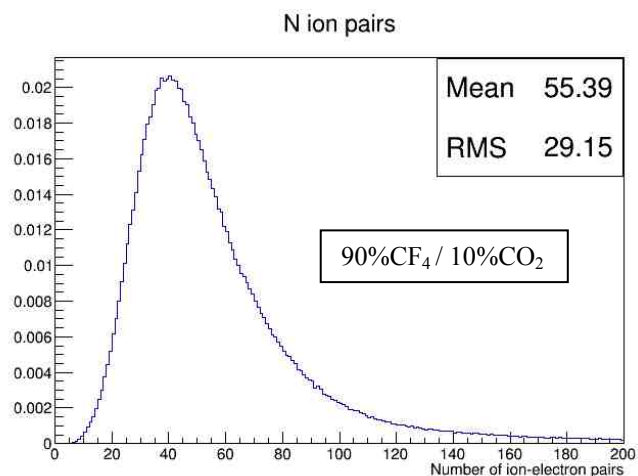


Fig. 3. Ion-pair distributions for three simulated gas mixtures. Normalized histograms, 10⁶ histories each.

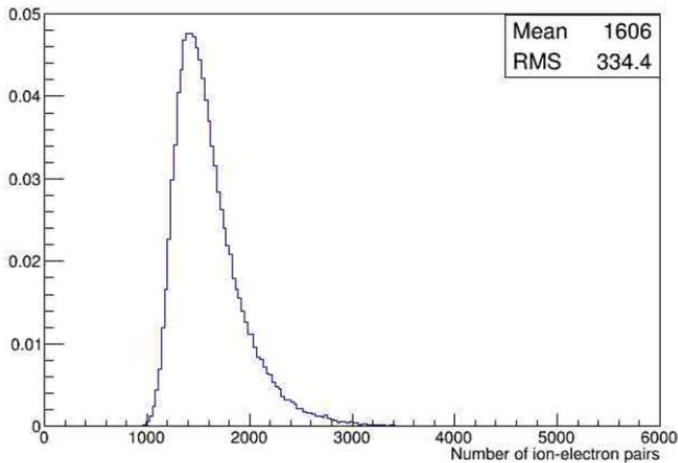


Fig. 4. Simulated number-of-ion-pairs distributions for a 375 MeV/n carbon ion beam, 2 mm gas gap, $\text{CF}_4\text{-CO}_2$ gas mixture, normalized, 10^6 histories.

B. Interference with the particle beam

A detector presence in a particle beam results in particle scattering due to interactions with the detector materials. Fig. 5 shows a 200 MeV proton needle beam spread due to multiple scattering in the detector materials and air on the proton path to the plane 20 cm downstream of the tracker (isocenter plane) for two PPS planes as in Fig. 1, compared to four 400 μm single-sided Si sensors (LLU pCT head scanner, [3]). One can see that proton beam scattering in PPS detector materials (including multiple Coulomb and large angle elastic scattering, as well as scattering caused by nuclear interactions) is less than that introduced by the Si micro-strip tracker.

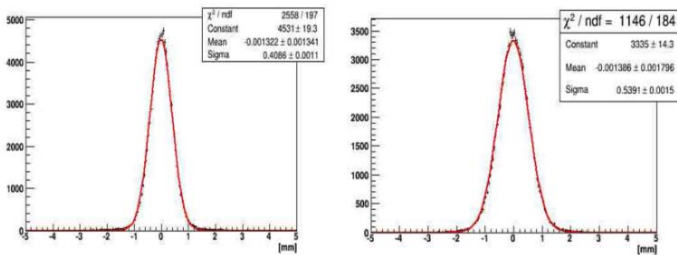


Fig. 5. 200 MeV proton beam broadening at a plane 20 cm downstream from the tracker caused by scattering in the detector materials. Left Pane – PPS tracker. Right Pane – Si micro-strip LLU pCT tracker.

The impact of non-uniformity in the PPS thickness introduced by the 30 μm thick patterned structure was studied simulating the PPS telescope with and without the patterned wall structure. It was found that for the 200 MeV protons, the energy at the PPS telescope exit and difference of range mean values was less than 0.5%, while the energy and proton range spread increase due to the patterned wall implementation was less than 0.01 MeV or $\approx 10 \mu\text{m}$ (see Fig. 6) – i.e., practically negligible for monitoring and imaging applications.

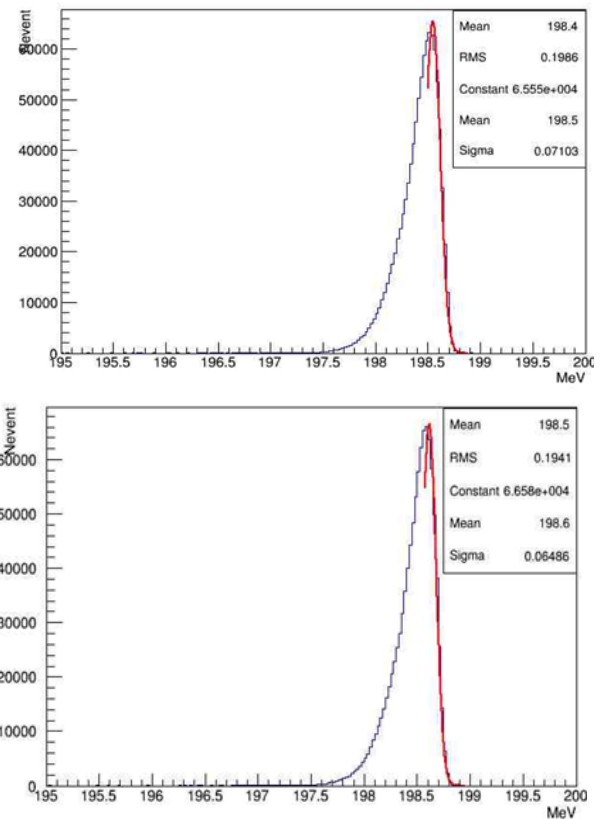
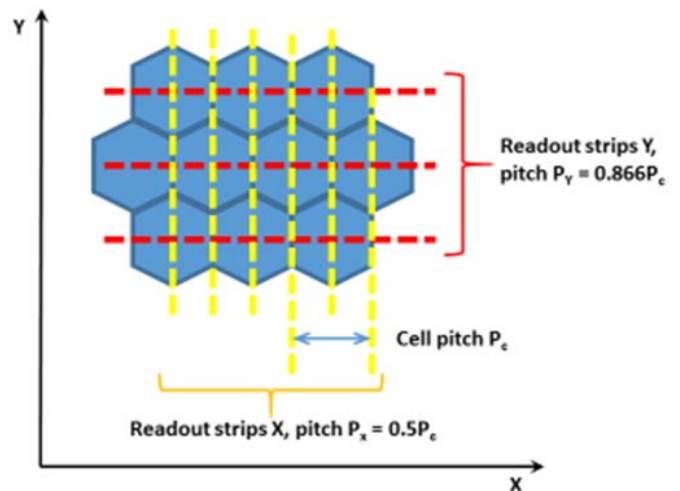


Fig. 6. Exit energy distributions for 200 MeV protons traversing the PPS tracker with (Upper Pane), and without (Lower Pane), patterned wall structure.

C. PPS spatial resolution

Fig. 7 shows the hexagon cell structure readout with readout strips going through centers of cell columns (X-strips) and rows (Y-strips). In this study, hexagon orientation was set with two cell sides parallel to the vertical axis, hence X and Y strip pitches were $P_x = P_c/2$ and $P_y = P_c \cos(30^\circ)$ (see Fig. 7).

Fig. 7. PPS cell and readout strip orientation.



Coordinates of particle hits were assigned as the geometrical center of the cell that fired, which means that the coordinate uncertainty was proportional to the readout pitch (see Fig. 8).

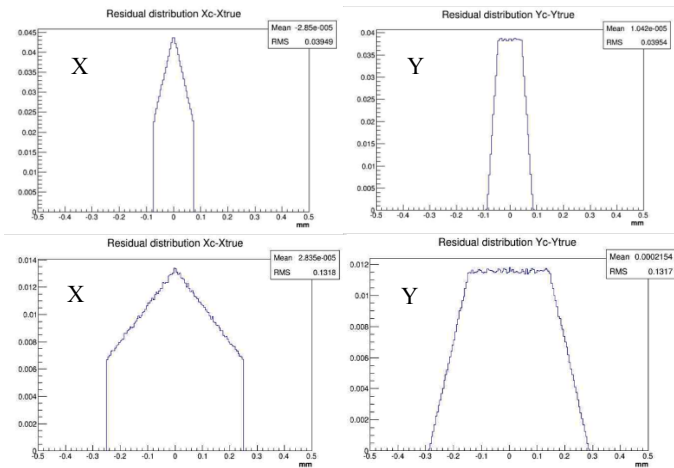


Fig. 8. X and Y coordinate residuals between real hit position and fired-cell center. Upper Row: cell pitch $P_c = 150 \mu\text{m}$, Lower Row: $P_c = 500 \mu\text{m}$.

Despite quite a difference in shape of the distribution of the X and Y residuals in Fig. 8, which reflects the hexagonal cell orientation with respect to the X and Y axis, the mean deviation (RMS), which can be approximated as $\text{RMS} = 0.2635 * P_c$, is the same for both coordinates. Because the hit coordinates are assigned to a strip center, the coordinate PPS response function yields discrete Gaussian distributions. When the track is extrapolated to a certain plane using these discrete values, the resulting track coordinate distribution in that plane is also discrete and broadened. Fig. 9 shows the intrinsic spatial resolution (i.e., difference between PPS telescope prediction and true position of the proton tracks) of the PPS telescope, calculated in a plane 20 cm downstream from the telescope. In this simulation, using a 200 MeV quasi-parallel (i.e., 1 mrad divergence) proton beam, the multiple coulomb scattering was turned off.

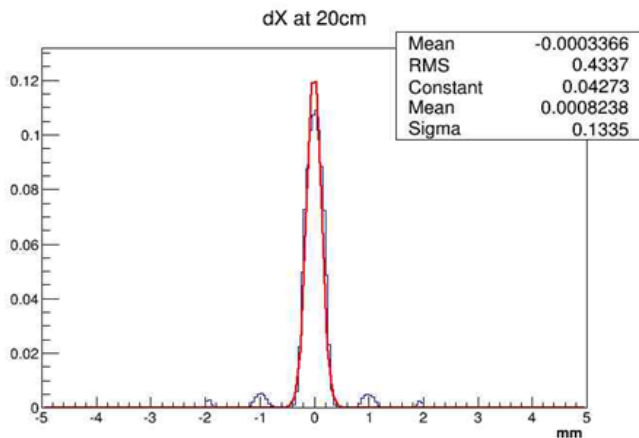


Fig. 9. Intrinsic spatial resolution of the PPS telescope, cell pitch $500 \mu\text{m}$.

D. Track reconstruction accuracy

The track reconstruction accuracy was evaluated at a plane 20 cm downstream from the tracker, i.e., presenting the isocenter plane orthogonal to the particle direction of a complete proton CT scanner. The simulation accounted for both particle scattering and detector spatial resolution. The resolution was estimated as the sigma of a Gaussian fitted to the distribution of the difference between actual particle position at the isocenter plane and the PPS telescope track

extrapolated from the PPS to that plane. The results are shown in Fig. 10.

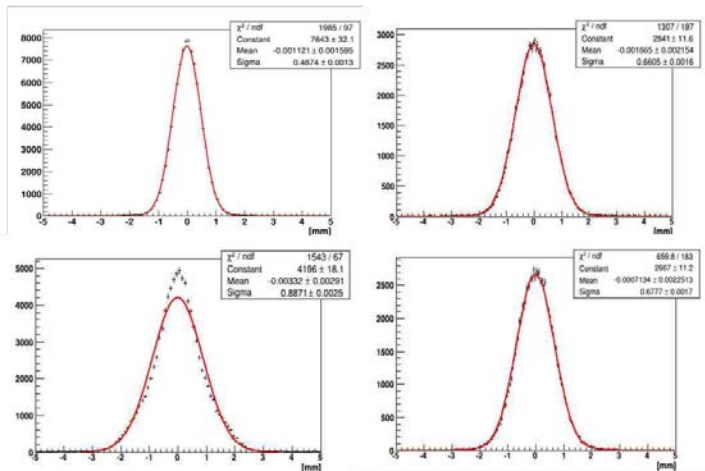


Fig. 10. 200 MeV proton track reconstruction accuracy at the plane 20 cm downstream from the tracker. Upper Pane: PPS detector with pitch of $150 \mu\text{m}$ (left) and $300 \mu\text{m}$ (right). Lower Pane: PPS with pitch of $500 \mu\text{m}$ (left), and Si micro-strip LLU pCT tracker with pitch of $238 \mu\text{m}$ (right).

A deviation from the Gaussian is clearly visible in the lower left plot of Fig. 10, where the track deviation due to scattering in the PPS material ($\approx 400 \mu\text{m}$) is of the order of the pitch ($500 \mu\text{m}$); therefore, the discrete response of the detector is not broadened enough to fit the Gaussian.

IV. CONCLUSION

The simulation study of a realistic PPS telescope design shows that this technology is comparable to, or better than, existing silicon sensors in terms of spatial resolution for proton imaging. Further improvement of the track reconstruction accuracy is possible by reducing the PPS substrate thickness. Fabrication of the simulated PPS telescope is currently underway at Integrated Sensors, LLC. In addition, PPS devices with substantially thinner substrates are under development.

ACKNOWLEDGMENT

This work was funded in part by the National Cancer Institute (NCI) under SBIR Phase-I grant 1R43CA183437 from the NIH.

REFERENCES

- [1] S. Agostinelli, *et al.*, "Geant4-a simulation toolkit", Nuclear Instruments and Methods in Physics Research, Section 506 A, pp. 250-303, 2003.
- [2] R. Ball, *et al.*, "Development of a plasma panel radiation detector", Nuclear Instruments and Methods in Physics Research, Section A, 764, pp.122-132, 2014.
- [3] H. F. W. Sadrozinski, *et al.*, "Development of a head scanner for proton CT," in Nuclear Instruments and Methods in Physics Research, Section A, 699, pp. 205-213, 2013.